Terahertz Memos

Memo 06

September 2010

The effect of the switch length and antenna width on the radiation quality factor and resonant frequency

Prashanth Kumar[1], Carl E. Baum[1], Kenneth F. McDonald[2],
Christos G. Christodoulou[1] and Edl Schamiloglu[1]

[1]University of New Mexico
Department of Electrical and Computer Engineering
Albuquerque, NM 87131

[2]Sci-Eng Solutions, LLC
3304 Lake Town Dr.
Columbia, MO 65203

Abstract

This paper explores the quality factor, Q, resonant frequency, f_0, and radiated power density, P_{rad}, as a function of the switch length, l_s, and antenna width, w, for a copper SWitched Oscillator (SWO) antenna above a copper ground plane with a (lossless) polyethylene substrate medium. Ranges for l_s and w are determined which yield the desired Q with maximum P_{rad}. Emperical relations for Q and f_0 as a function of l_s and w are obtained using curve fits.

1 Introduction

This paper investigates the effects of the switch length, l_s, and antenna width, w, on the radiation quality factor, Q, the resonant frequency, f_0, and the radiated power density, P_{rad}, for a copper SWO above a copper ground plane with a lossless polyethylene substrate medium. Unlike the parameter h (substrate height) investigated in previous papers [1, 2], the effects of l_s and w on Q and f_0 are too complicated to assess theoretically. Analytical approximations in [3] simplified the problem by assuming that the switch gap length was much less than the antenna length, $l_s \ll l_a$, and that $w = \lambda/4$.

The switch length is important as it ultimately dictates the requirements of the laser beam incident on the photoconductor. The antenna width is important as it determines the modes that can be sustained by the radiator. The primary aim in optimizing w is to eliminate unwanted modes to obtain the desired Q and maximize P_{rad}.

2 Simulation

2.1 Q, f_0, and P_{rad} as a function of l_s

2.1.1 Setup

The setup, probe placements and CST simulation parameters are identical to [4] except that the switch length, l_s, is varied from $l_s = \lambda/50$ to $l_s = \lambda/5$. Also, the width of the antenna is fixed at $w = l_a/2 = \lambda/4$, i.e., unlike the simulations in [4], $w \neq (l_a - l_s)/2$. Lossless polyethylene, $\epsilon_{\text{rs}} = 2.25$, is used as the substrate medium. The height of the SWO above the ground plane, h, is (arbitrarily) fixed at $h = \lambda/8 = (2/3)\lambda_0/8 = 50$ μm. The dimensions of the SWO, substrate and ground plane are summarized in Table. 1.

Table 1: Dimensions for a copper SWO above a copper ground plane with a substrate medium and varying switch length.

Parameter	Dimensions (μm)
Antenna length, l_a	$\lambda/2 = 200$
Antenna height (thickness)	1
Switch length, l_s	$\lambda/50 \leq l_s \leq \lambda/5$
Antenna width, w	$l_a/2 = 100$
Height of substrate, h	$\lambda/8 = 50$
Length of substrate and ground plane	$3\lambda = 1200$
Width of substrate and ground plane	$3\lambda = 1200$
Height of ground plane (thickness)	1

2.1.2 Results

Table. 2 summarizes the peak electric field ($E_{\max}$), resonant frequency (f_0) and quality factor (Q) as a function of l_s. One observes that both f_0 and Q change with l_s.

Table 2: Variation of the peak electric field ($E_{\max}$), resonant frequency (f_0) and quality factor (Q) with the switch length (l_s).

l_s/λ	$E_{\max}$ (V/m)	f_0 (THz)	Q
0.025	35.162	0.367	19.809
0.033	32.51	0.357	22.564
0.050	27.993	0.339	27.597
0.075	23.097	0.32	34.417
0.100	19.374	0.305	40.164
0.125	16.473	0.294	45.25
0.150	14.233	0.284	49.605
0.200	10.987	0.272	54.709

Figure 2.1 and Fig. 2.2 show a plot of Q and f_0 as a function of l_s. As in [4], a generic function of the form

$$\alpha\left(h, l_a, \epsilon_{\rm rs}, \frac{l_s}{\lambda}, w\right) = \beta(l_a, h, \epsilon_{\rm rs}, w)\left[\frac{l_s}{\lambda}\right]^{\xi} \tag{2.1}$$

is chosen to obtain an emperical relation between Q, f_0 and l_s. Note that α and β are, in general, also a function of l_a, h, $\epsilon_{\rm rs}$ and w. Since $l_a, h, \epsilon_{\rm rs}$ and w are fixed, Table. 1, α is only a function of l_s/λ and β is constant. For $\alpha = Q$ in (2.1), the coefficients are $\beta \approx 125$ and $\xi \approx 0.5$, i.e.,

$$Q\left(\frac{l_s}{\lambda}\right) \approx 125\sqrt{\frac{l_s}{\lambda}}, \quad \frac{1}{50} \leq \frac{l_s}{\lambda} \leq \frac{1}{5}, \tag{2.2}$$

For $\alpha = f_0$ in (2.1), $\beta = 0.22$ and $\xi = -0.15$, i.e.,

$$f_0\left(\frac{l_s}{\lambda}\right) \approx 0.22\left[\frac{l_s}{\lambda}\right]^{-0.15}, \quad \frac{1}{50} \leq \frac{l_s}{\lambda} \leq \frac{1}{5}. \tag{2.3}$$

The fits for Q and f_0 in Fig. 2.1 and Fig. 2.2 are not as good as than those in [4]. Individual plots for the far-field electric field in the time and frequency domains for each simulation data point in Table. 2 are given in Appendix-I.

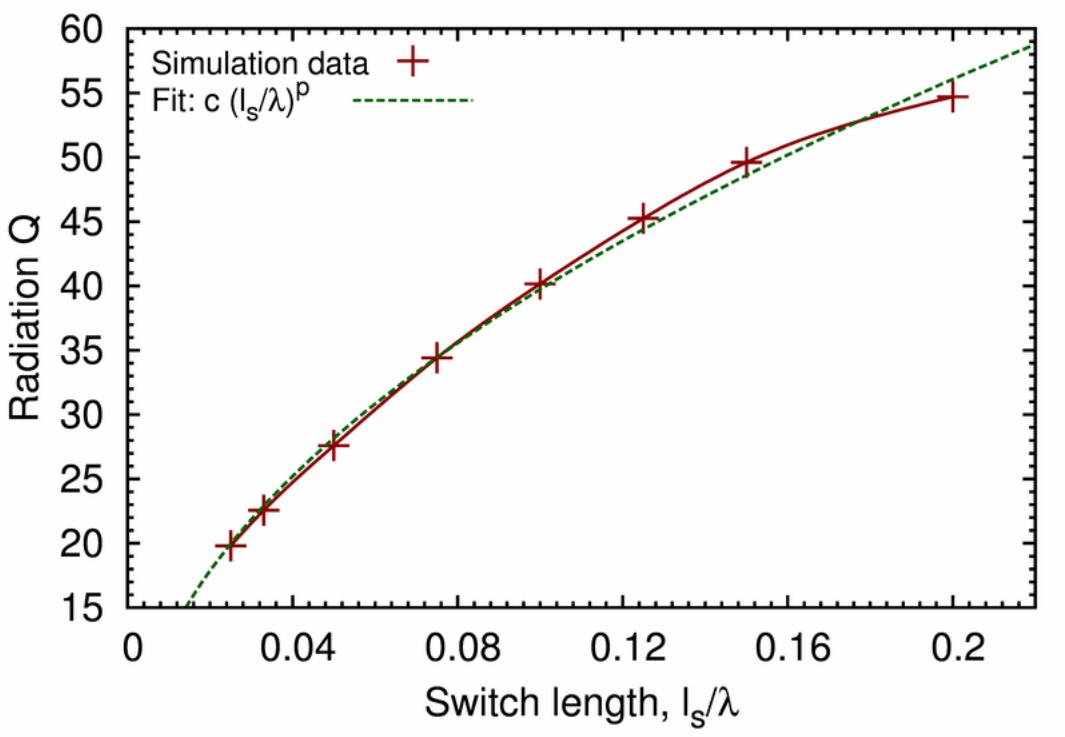

Figure 2.1: The quality factor, Q, as a function of the switch length, l_s. A function is fit to the results to obtain an emperical relation between Q and l_s.

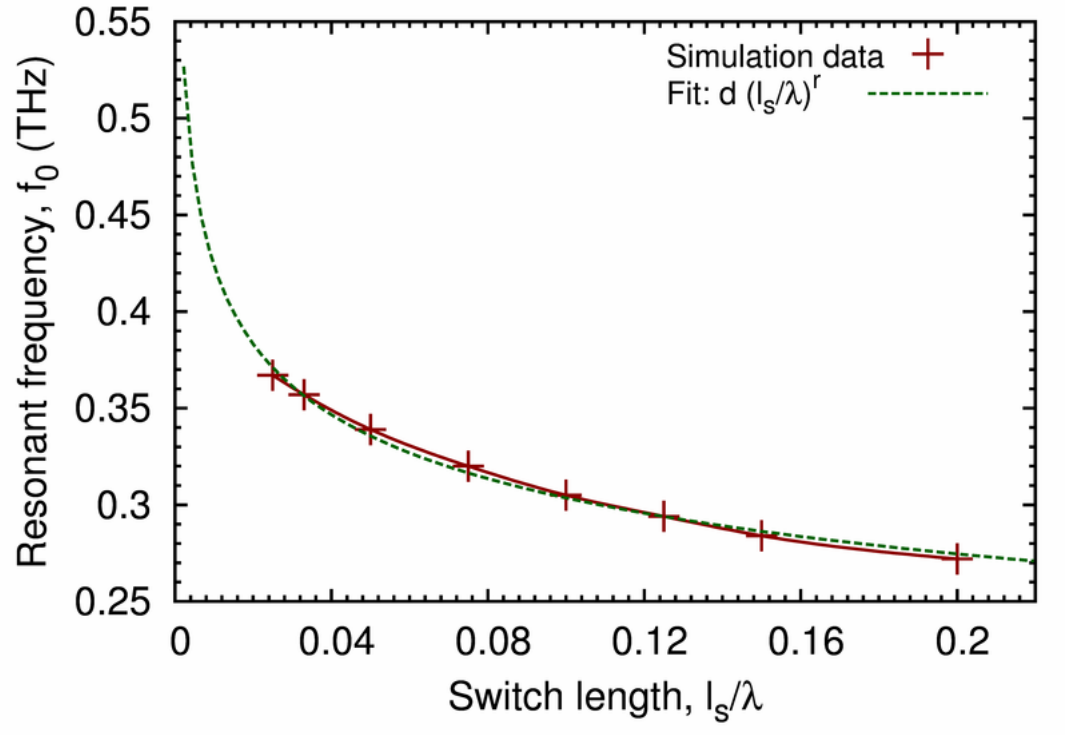

Figure 2.2: The resonant frequency, f_0, as a function of the switch length, l_s. A function is fit to the results to obtain an emperical relation between f_0 and l_s.

The results in Table 2 are interesting as they suggest that for a fixed $h, \epsilon_{\rm rs}$ and w, the Q can be increased by increasing the switch length. As in [4], we must ensure that the time taken for the radiated electric field to decay to zero, τ, is less than 100 ps. Imposing this second constraint, by examining the far-field electric field responses in Appendix-I, we have

$$0.025 \leq \frac{l_s}{\lambda} \leq 0.075 \Rightarrow 20 \leq Q \leq 35. \tag{2.4}$$

However, compared to varying h, [4], varying l_s to increase the Q has the disadvantage that the resonant frequency also changes, since f_0 is also a function of l_s. Moreover, we have from [4],

$$0.05 \leq \frac{h}{\lambda} \leq 0.100 \Rightarrow 25 \leq Q \leq 50, \tag{2.5}$$

i.e., a higher Q is obtained by varying h than that obtained by varying l_s. Nevertheless, increasing l_s may be attractive from an experimental perspective as the voltage hold-off is dictated by l_s and not h, since, typically, $l_s \ll h$. Increasing l_s would therefore imply a higher input voltage, which is desirable.

The peak radiated power densities, at $r = 1$ m in the $\theta = 90^\circ$ plane, at the resonant frequencies, were found to be less than 30 mW/m^2 for all $0.05 \leq l_s/\lambda \leq 0.2$. The far-field radiated power density patterns, normalized to 40 dB, for various l_s, at the respective resonant frequencies, were found to be dipolar.

2.2 Q, f_0, and $P_{\rm rad}$ as a function of w

2.2.1 Setup

The setup, probe placements and CST simulation parameters are identical to [4] except that the antenna width, w, is varied from $w = \lambda/20$ to $w = \lambda$. Lossless polyethylene, $\epsilon_{\rm rs} = 2.25$, is used as the substrate medium. The height of the SWO above the ground plane, h, is (arbitrarily) fixed at $h = \lambda/8 = (2/3)\lambda_0/8 = 50$ μm. The dimensions of the SWO, substrate and ground plane are summarized in Table. 3.

2.2.2 Results

Table. 4 summarizes the peak electric field ($E_{\rm max}$), resonant frequency (f_0) and quality factor (Q) as a function of w/λ. One observes that both f_0 and Q change with w.

Figure 2.3 and Fig. 2.4 show a plot of Q and f_0 as a function of w. There is a large variation of both, the Q and f_0 with w. A generic function of the form

$$\alpha\left(h, l_a, \epsilon_{\rm rs}, \frac{w}{\lambda}, l_s\right) = \beta(h, \epsilon_{\rm rs}, l_s)\left[\frac{w}{\lambda}\right]^{\xi} + \zeta(h, \epsilon_{\rm rs}, l_s) \tag{2.6}$$

is chosen to obtain an emperical relation between Q, f_0 and w. Again, α, β and ζ are, in general, also a function of l_a, h, $\epsilon_{\rm rs}$ and l_s. Since $l_a, h, \epsilon_{\rm rs}$ and l_s are fixed, Table. 3, α is only a function of w/λ while β and ζ are constant. For $\alpha = Q$ in (2.6), the coefficients are $\beta \approx 36, \xi \approx 1.35$ and $\zeta \approx 14$, i.e.,

$$Q\left(\frac{w}{\lambda}\right) \approx 36\left[\frac{w}{\lambda}\right]^{1.35} + 14, \quad \frac{1}{20} \leq \frac{w}{\lambda} \leq 1, \tag{2.7}$$

Table 3: Dimensions for a copper SWO above a copper ground plane with a substrate medium and varying antenna width.

Parameter	Dimensions (μm)
Antenna length, l_a	$\lambda/2 = 200$
Antenna height (thickness)	1
Switch length, l_s	$\lambda/50 = 8$
Antenna width, w	$\lambda/20 \leq w \leq \lambda$
Height of substrate, h	$\lambda/8 = 50$
Length of substrate and ground plane	$3\lambda = 1200$
Width of substrate and ground plane	$3\lambda = 1200$
Height of ground plane (thickness)	1

Table 4: Variation of the peak electric field ($E_{\max}$), resonant frequency (f_0) and quality factor (Q) with the switch length (w).

w/λ	$E_{\max}$ (V/m)	f_0 (THz)	Q
0.050	16.919	0.466	15.553
0.100	22.174	0.437	15.502
0.125	24.9	0.424	15.733
0.150	27.911	0.413	16.074
0.200	33.14	0.392	17.023
0.250	36.116	0.378	18.039
0.300	38.82	0.356	20.059
0.350	39.643	0.34	22.066
0.400	39.593	0.324	24.03
0.450	39.051	0.31	26.295
0.500	38.007	0.295	28.277
0.625	33.961	0.266	33.444
0.750	28.764	0.24	38.214
0.875	23.951	0.217	44.363
1.000	20.246	0.199	48.615

For $\alpha = f_0$ in (2.6), $\beta = -0.35, \xi \approx 0.5$ and $\zeta \approx 0.6$, i.e.,

$$f_0\left(\frac{w}{\lambda}\right) \approx -0.35\sqrt{\frac{w}{\lambda}} + 0.6, \quad \frac{1}{20} \leq \frac{w}{\lambda} \leq 1. \tag{2.8}$$

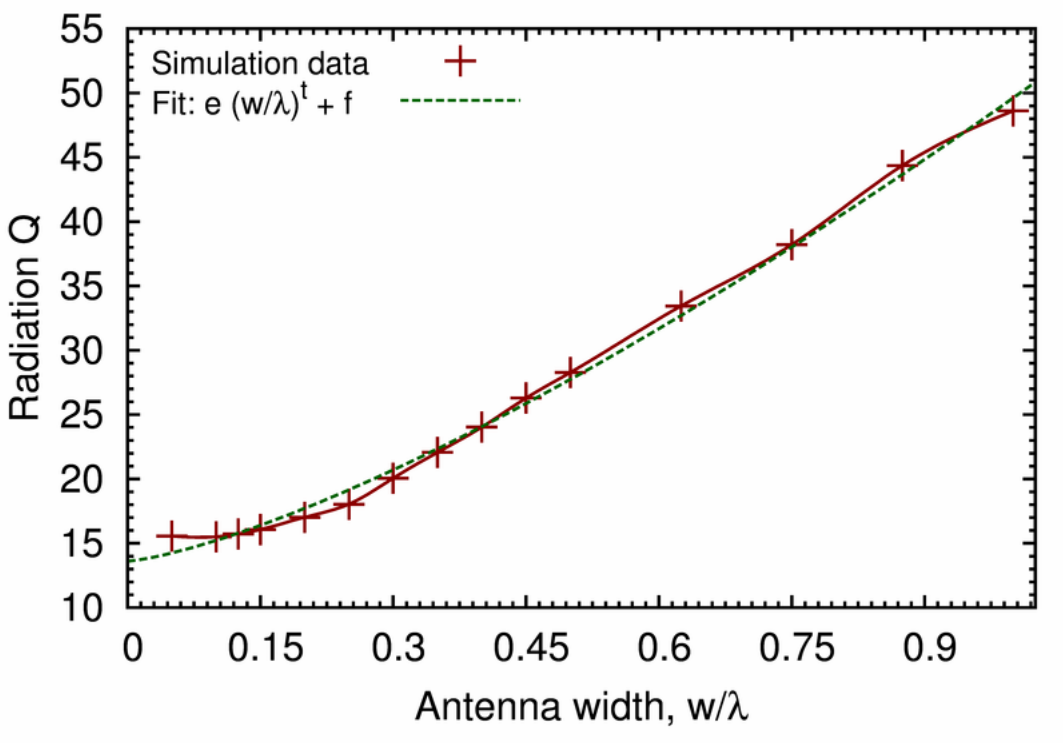

Figure 2.3: The quality factor, Q, as a function of the switch length, w. A function is fit to the results to obtain an emperical relation between Q and w.

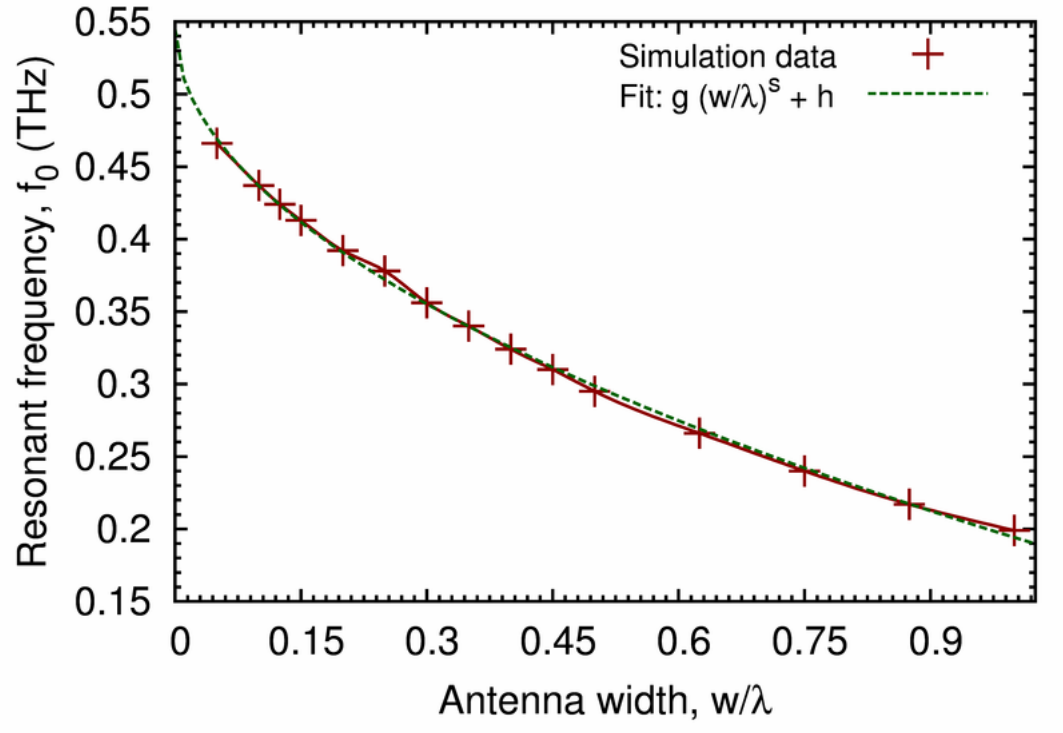

Figure 2.4: The resonant frequency, f_0, as a function of the antenna width, w. A function is fit to the results to obtain an emperical relation between f_0 and w.

Individual plots for the far-field electric field in the time and frequency domains for the most important simulation data points in Table. 4 are given in Appendix-II. Imposing the constraint of the decay time of the radiated electric field, i.e., $\tau \leq 100$ ps, the width of the antenna is constrained as $w < \lambda/2$.

The radiated power densities, at $r = 1$ m in the $\theta = 90^\circ$ plane, at the resonant frequencies for various w are compared in Fig. 2.5. The radiation Qs and the peak radiated power densities (at $r = 1$ m) for various w are compared in Fig. 2.6. It is clear that the radiated power density is maximum at $w = \lambda/8$ and $w = \lambda/2$. At these widths, the peak radiated power is approximately 10 times that at $w = \lambda/4$. Since $w < \lambda/2$, the most suitable choice for the antenna width is $w = \lambda/8$. The Q of the system can then be increased by increasing the switch length, l_s, as in Sec. 2.1.2.

The far-field radiated power density patterns, normalized to 40 dB, for various w, at the respective resonant frequencies, are compared in Fig. 2.7. Again, the radiation patterns are dipolar.

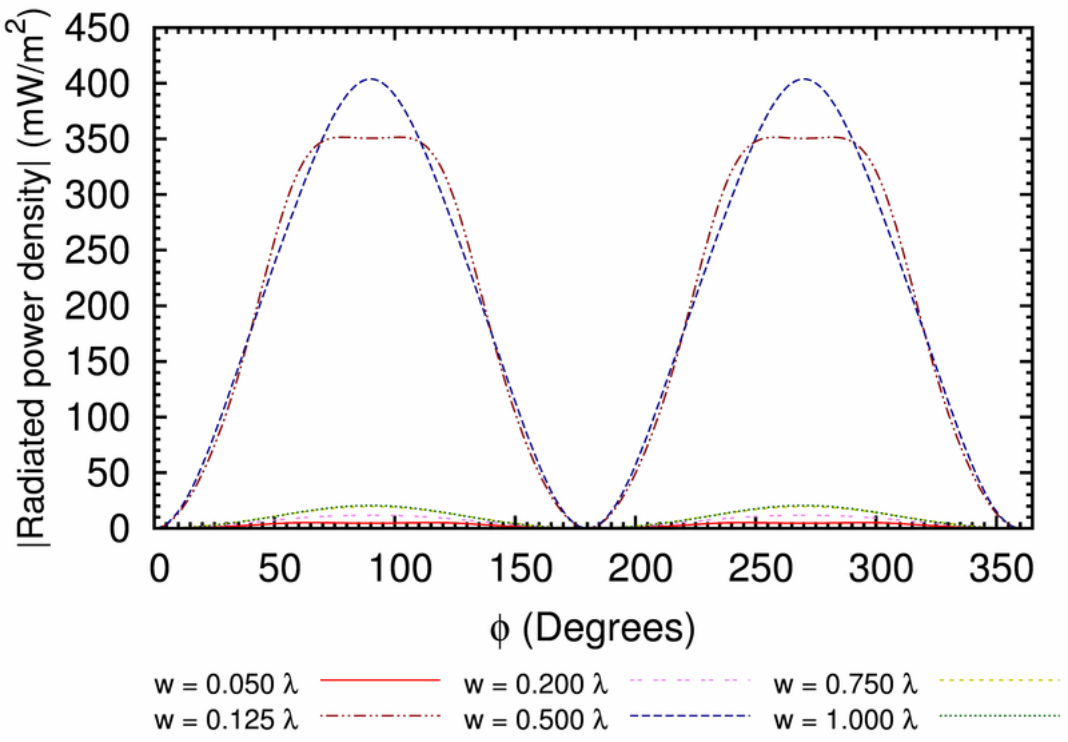

Figure 2.5: Comparison of the radiated power density, at $r = 1$ m in the $\theta = 90^\circ$ plane, at the resonant frequencies for various antenna widths, w.

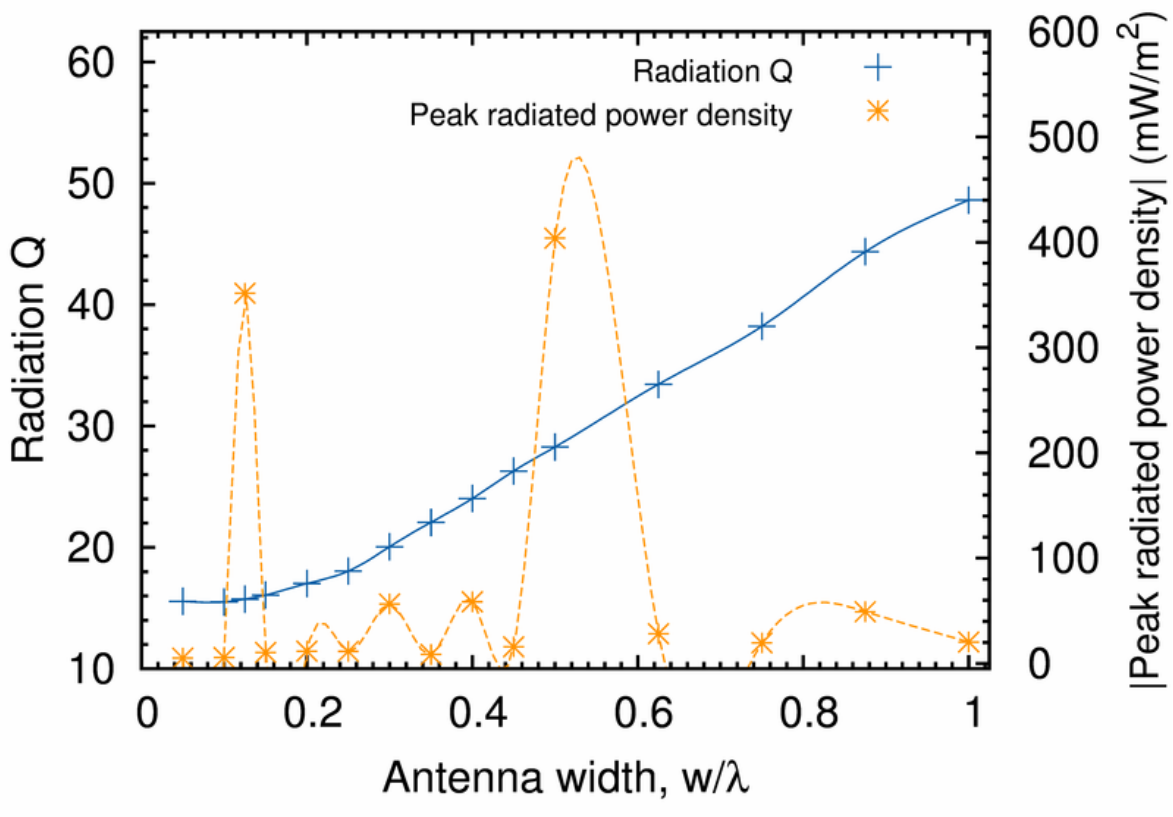

Figure 2.6: Comparison of the quality factor and the peak radiated power density (at $r = 1$ m) as a function of the antenna width.

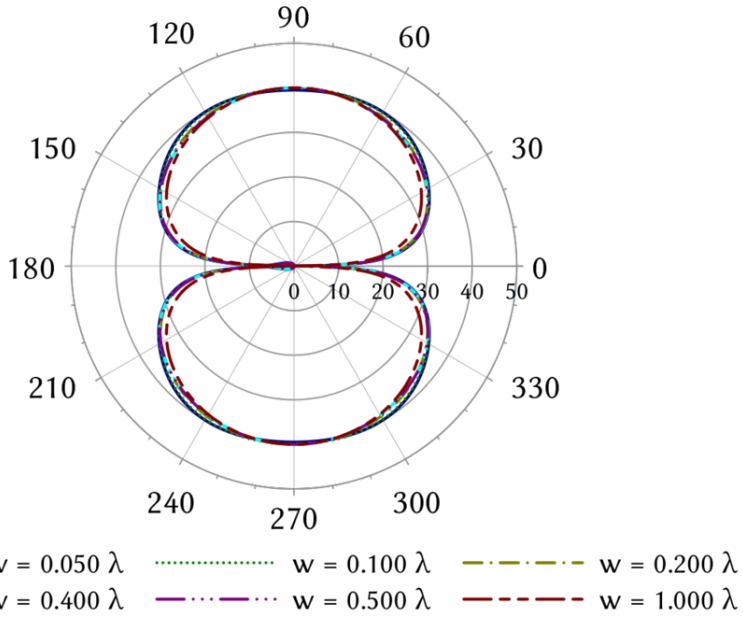

Figure 2.7: Normalized (to 40 dB) polar plot of the radiated power density (in the $\theta = 90°$ plane), at the resonant frequencies for various w, to ascertain the shape of the radiation pattern. The radial scale is 10 dB/div.

3 Conclusions

The radiation Q and the resonant frequency, f_0, are both dependent on the switch length, l_s. For $w = \lambda/4$, $l_a = \lambda/2$, $\epsilon_{\rm rs} = 2.25$ (lossless) and $h = \lambda/8$, we have the following emperical relations,

- $Q\left(\frac{l_s}{\lambda}\right) \approx 125\sqrt{\frac{l_s}{\lambda}}, \quad \frac{1}{50} \leq \frac{l_s}{\lambda} \leq \frac{1}{5},$
- $f_0\left(\frac{l_s}{\lambda}\right) \approx 0.22\left[\frac{l_s}{\lambda}\right]^{-0.15}, \quad \frac{1}{50} \leq \frac{l_s}{\lambda} \leq \frac{1}{5},$

i.e., for a fixed h, the Q can be increased by increasing the switch length. For $\tau \leq 100$ ps the range of l_s is reduced to $0.025 \leq \frac{l_s}{\lambda} \leq 0.075$.

Compared to h, l_s and $\epsilon_{\rm rs}$, the antenna width, w, is the most important parameter as it *significantly* influences the radiated power density. The radiation Q and the resonant frequency are both dependent on w.

For $l_s = \lambda/50$, $l_a = \lambda/2$, $\epsilon_{\rm rs} = 2.25$ (lossless) and $h = \lambda/8$, we have the following emperical relations,

- $Q\left(\frac{w}{\lambda}\right) \approx 36\left[\frac{w}{\lambda}\right]^{1.35} + 14, \quad \frac{1}{20} \leq \frac{w}{\lambda} \leq 1,$
- $f_0\left(\frac{w}{\lambda}\right) \approx -0.35\sqrt{\frac{w}{\lambda}} + 0.6, \quad \frac{1}{20} \leq \frac{w}{\lambda} \leq 1,$

For $\tau \leq 100$ ps, the width is constrained as $w < \lambda/2$. The radiated peak power densities are maximum, about 10 times that at $w = \lambda/4$, at $w = \lambda/8$ and $w = \lambda/2$. Since, $w < \lambda/2$, the most practical choice for high radiated power is $w = \lambda/8$. The Q can then be increased by increasing the switch length, l_s.

References

[1] Prashanth Kumar, Carl E. Baum, D. R. Grischkowsky, Kenneth F. McDonald, Christos G. Christodoulou and Edl Schamiloglu, "Comparison of experimental and numerical simulation results for the 5-10-5 max1 antenna," *Terahertz Memo 3*, Aug. 2010.

[2] Prashanth Kumar, Carl E. Baum, Kenneth F. McDonald, Christos G. Christodoulou and Edl Schamiloglu, "Investigation of the skin-effect losses in a copper swo antenna above a copper ground plane," *Terahertz Memo 4*, Aug. 2010.

[3] C. E. Baum and P. Kumar, "Maximizing Energy in Terahertz Pulse Radiation from a Switched Oscillator," *Sensor and Simulation Note XX*, July 2010.

[4] Prashanth Kumar, Carl E. Baum, Kenneth F. McDonald, Christos G. Christodoulou and Edl Schamiloglu, "Optimization of the substrate height for a copper swo radiator above a copper ground plane," *Terahertz Memo 5*, Sept. 2010.

Appendix - I

Radiated far-field electric fields, in the time and frequency domains, as a function of the switch length, l_s, with a lossless polyethylene substrate medium.

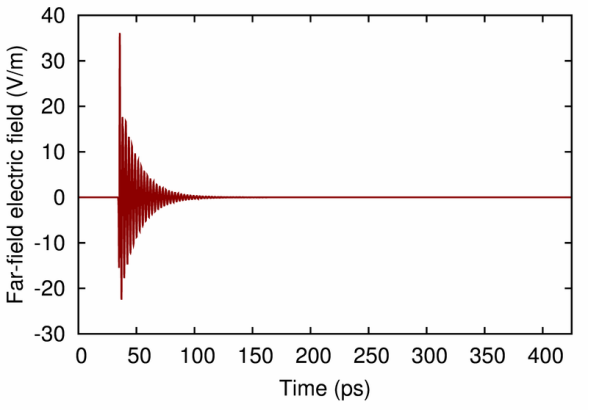

(a) $l_s = 0.020\lambda$.

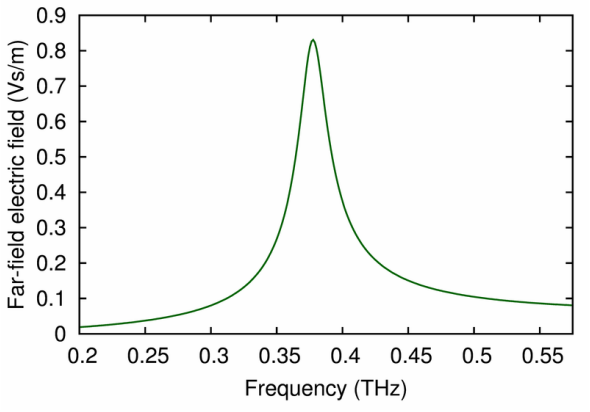

(b) $l_s = 0.020\lambda$.

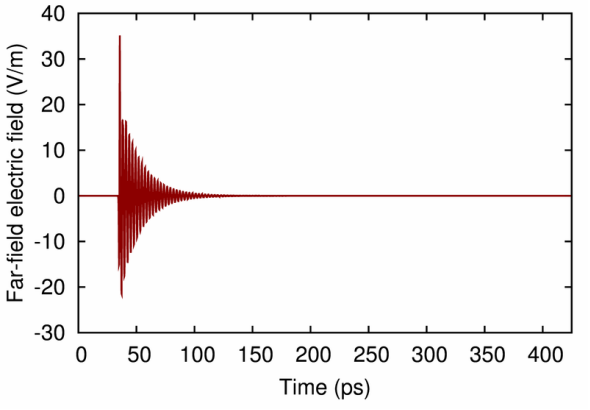

(c) $l_s = 0.025\lambda$.

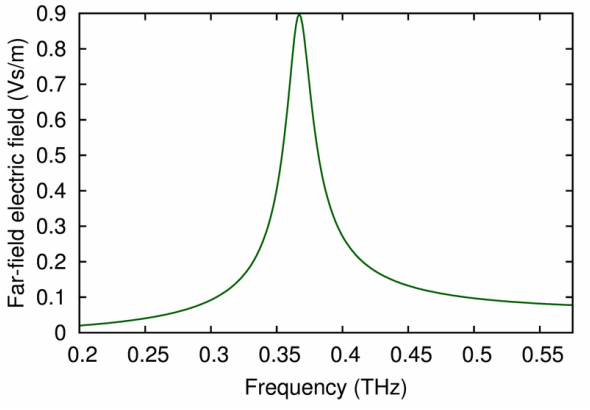

(d) $l_s = 0.025\lambda$.

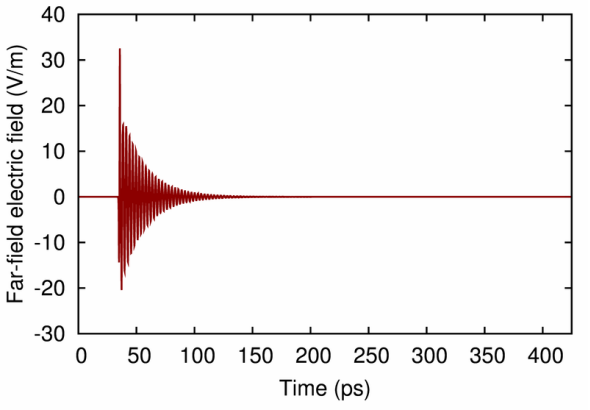

(e) $l_s = 0.033\lambda$.

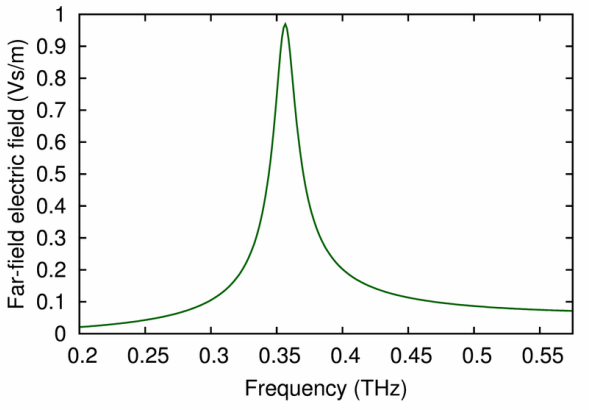

(f) $l_s = 0.033\lambda$.

Figure 3.1: Radiated far-field electric field pulse in the time and frequency domains for $l_s = 0.020\lambda, 0.025\lambda$ and $l_s = 0.033\lambda$.

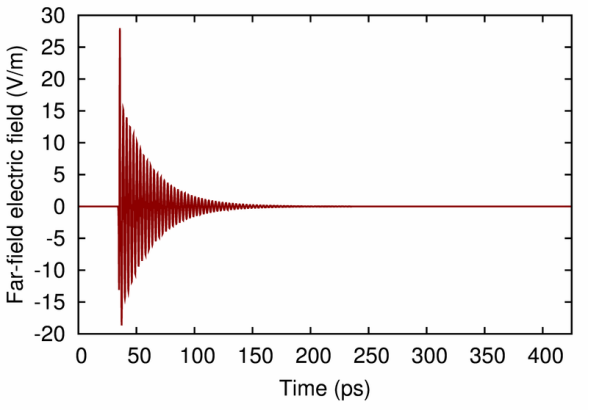

(a) $l_s = 0.050\lambda$.

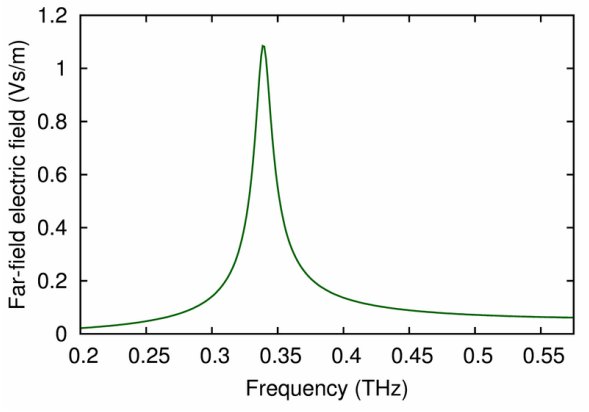

(b) $l_s = 0.050\lambda$.

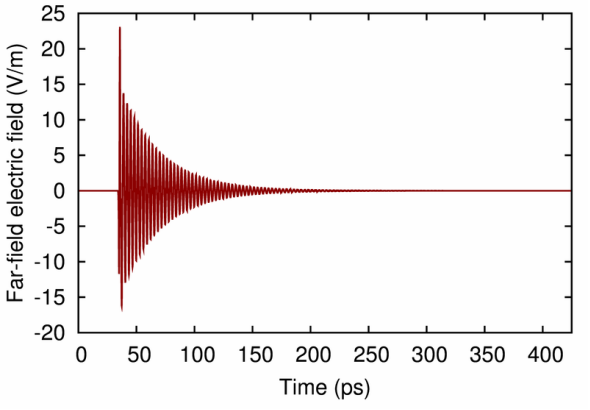

(c) $l_s = 0.075\lambda$.

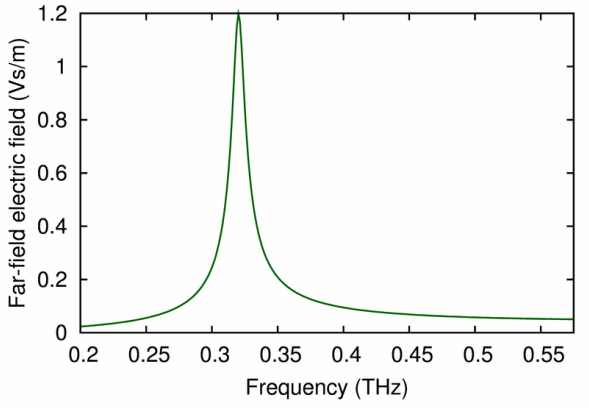

(d) $l_s = 0.075\lambda$.

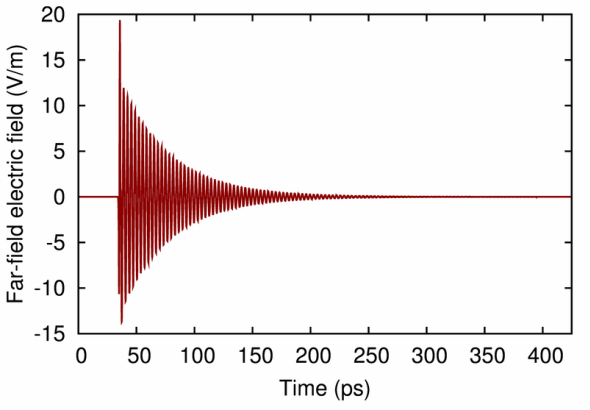

(e) $l_s = 0.100\lambda$.

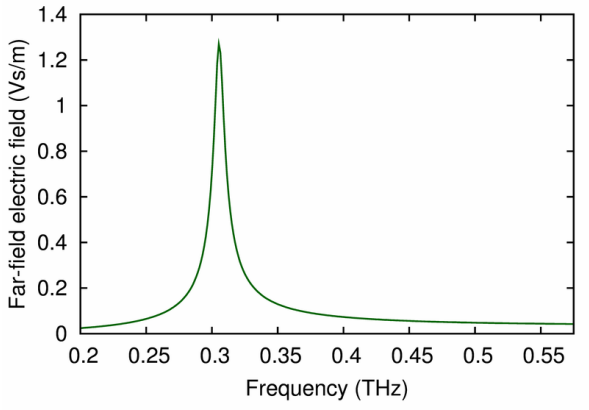

(f) $l_s = 0.100\lambda$.

Figure 3.2: Radiated far-field electric field pulse in the time and frequency domains for $l_s = 0.050\lambda, 0.075\lambda$ and $l_s = 0.100\lambda$.

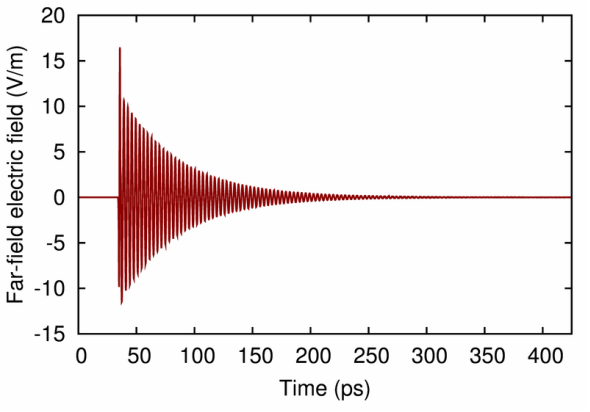

(a) $l_s = 0.125\lambda$.

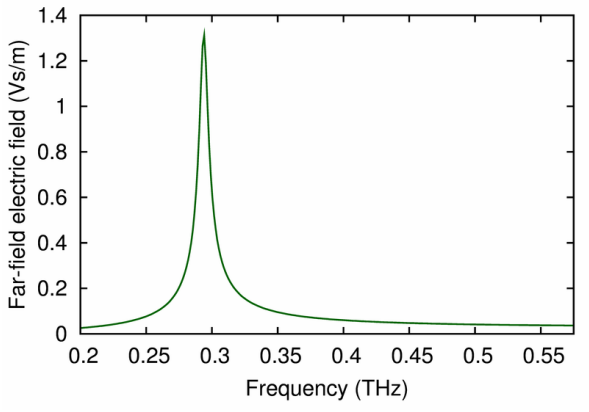

(b) $l_s = 0.125\lambda$.

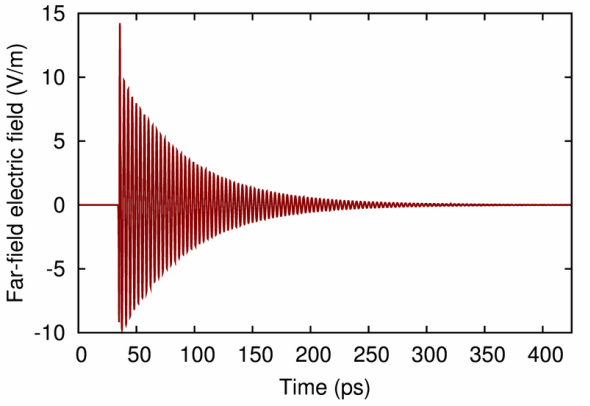

(c) $l_s = 0.150\lambda$.

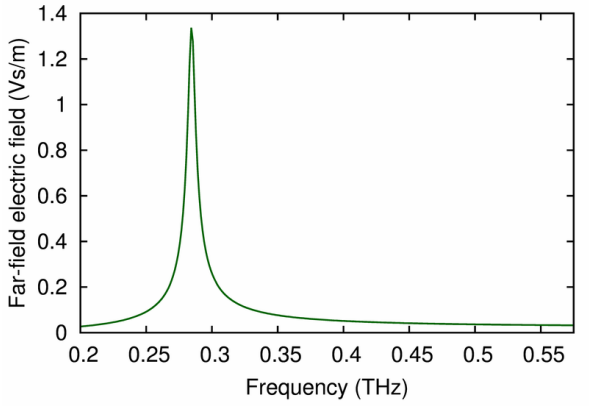

(d) $l_s = 0.150\lambda$.

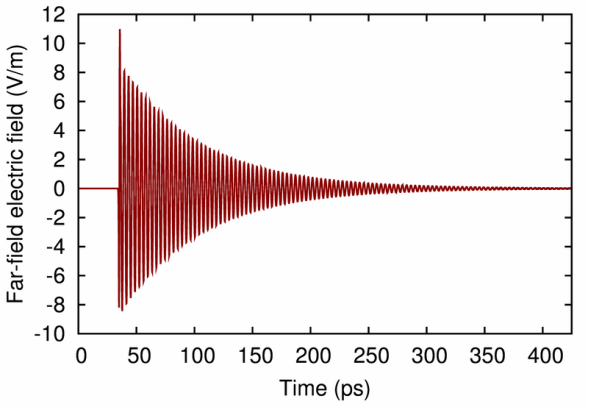

(e) $l_s = 0.200\lambda$.

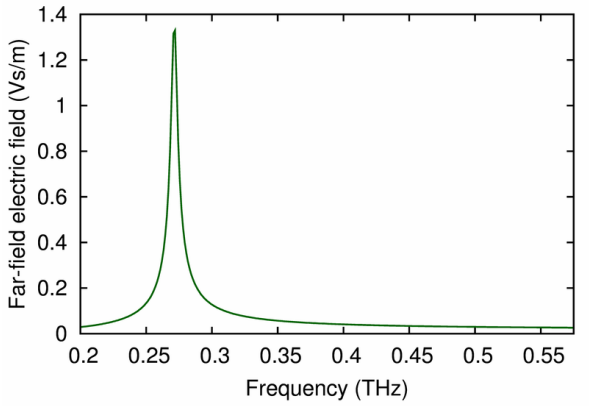

(f) $l_s = 0.200\lambda$.

Figure 3.3: Radiated far-field electric field pulse in the time and frequency domains for $l_s = 0.125\lambda, 0.150\lambda$ and $l_s = 0.200\lambda$.

Appendix - II

Radiated far-field electric fields, in the time and frequency domains, as a function of the antenna width, w, with a lossless polyethylene substrate medium.

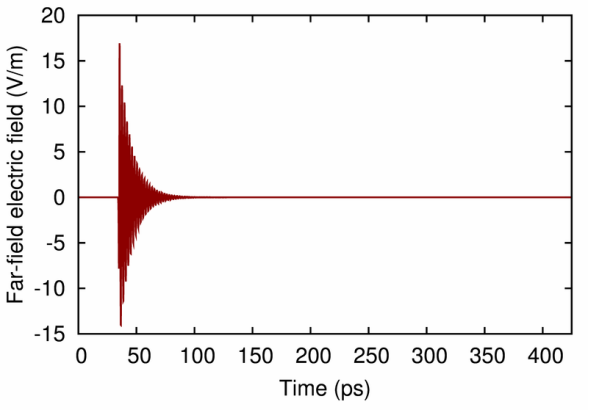

(a) $w = 0.050\lambda$.

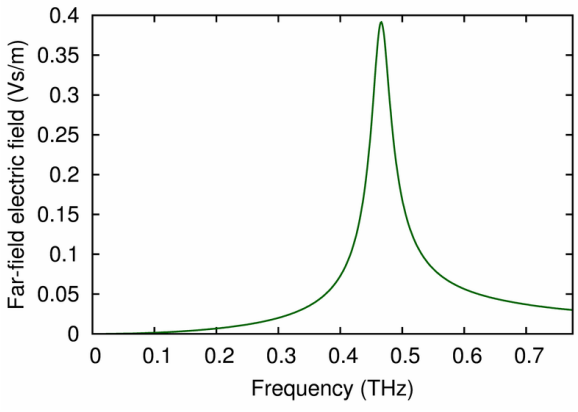

(b) $w = 0.050\lambda$.

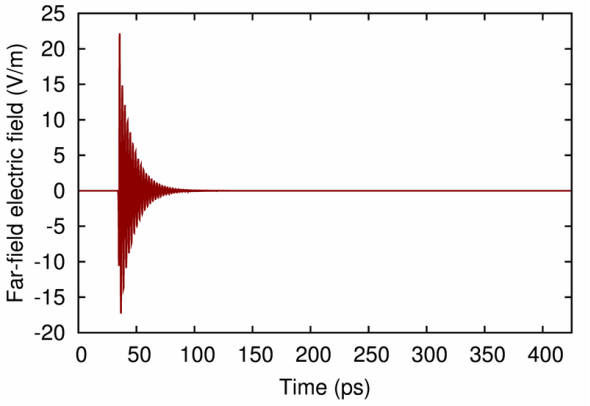

(c) $w = 0.100\lambda$.

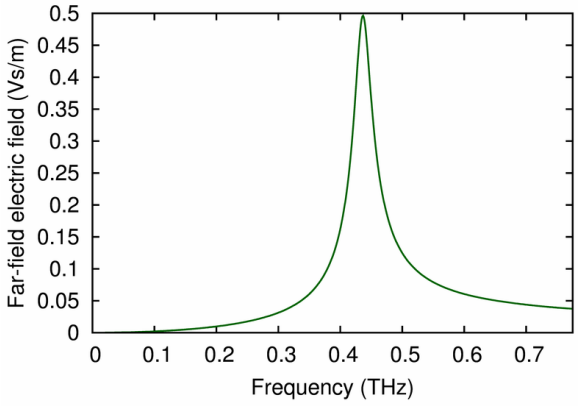

(d) $w = 0.100\lambda$.

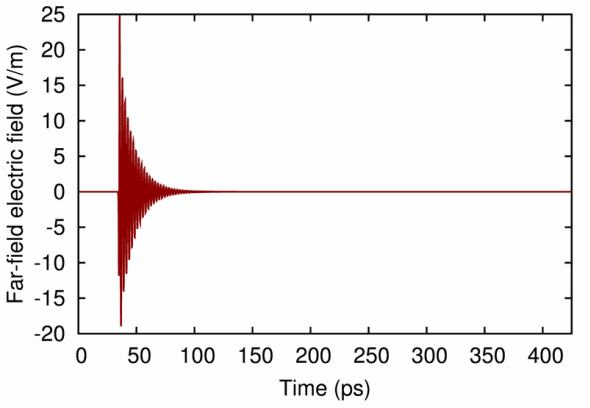

(e) $w = 0.125\lambda$.

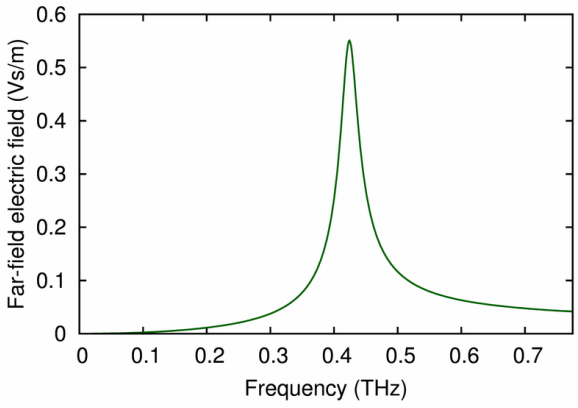

(f) $w = 0.125\lambda$.

Figure 3.4: Radiated far-field electric field pulse in the time and frequency domains for $w = 0.050\lambda, 0.100\lambda$ and $w = 0.125\lambda$.

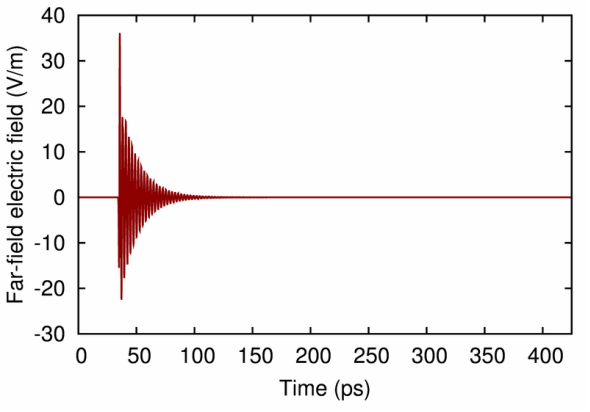

(a) $w = 0.250\lambda$.

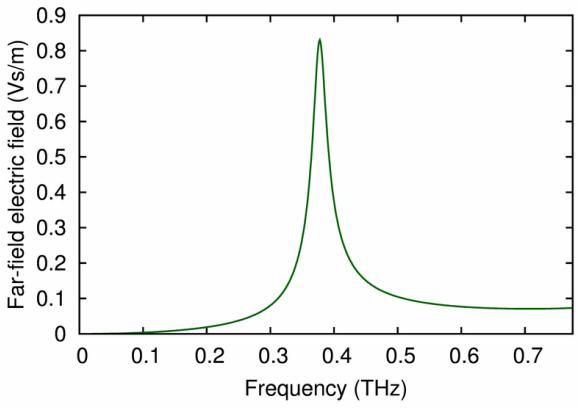

(b) $w = 0.250\lambda$.

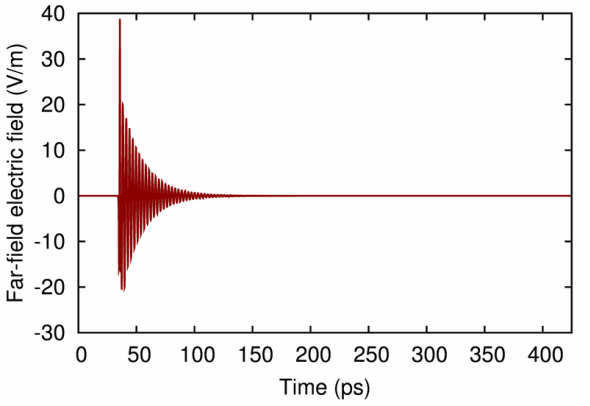

(c) $w = 0.300\lambda$.

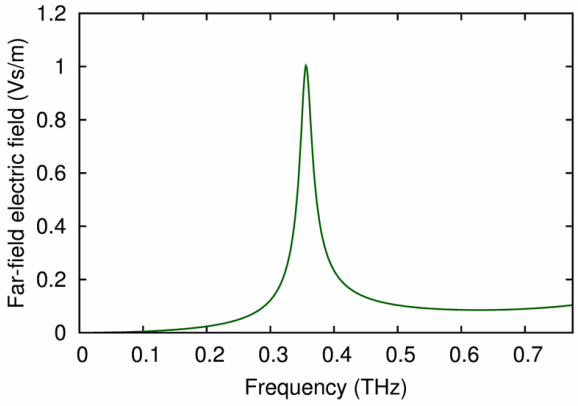

(d) $w = 0.300\lambda$.

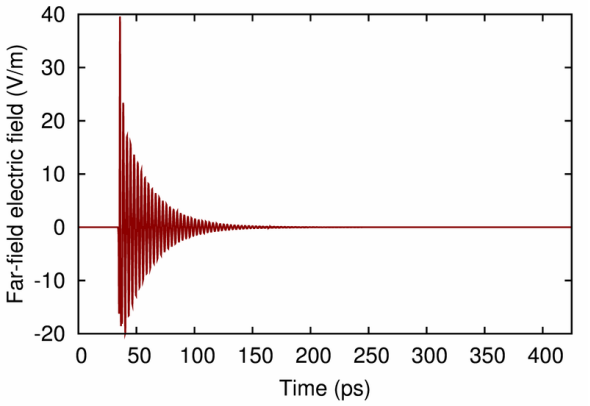

(e) $w = 0.400\lambda$.

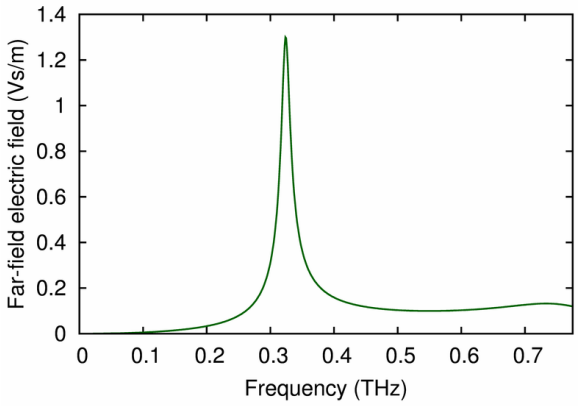

(f) $w = 0.400\lambda$.

Figure 3.5: Radiated far-field electric field pulse in the time and frequency domains for $w = 0.250\lambda, 0.300\lambda$ and $w = 0.400\lambda$.

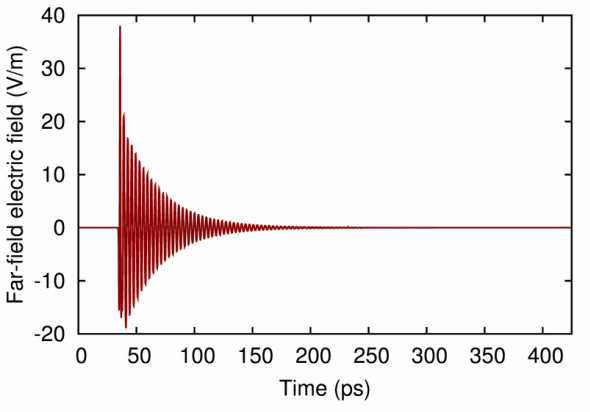

(a) $w = 0.500\lambda$.

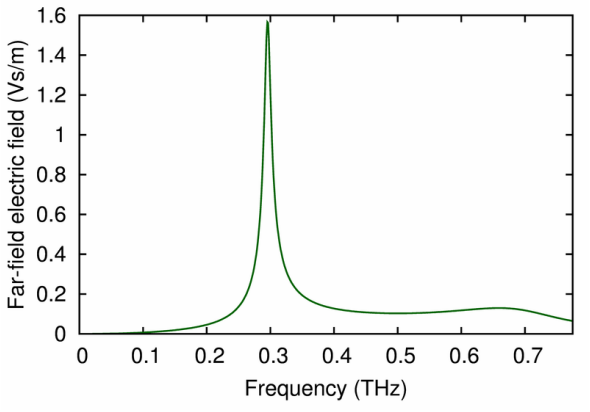

(b) $w = 0.500\lambda$.

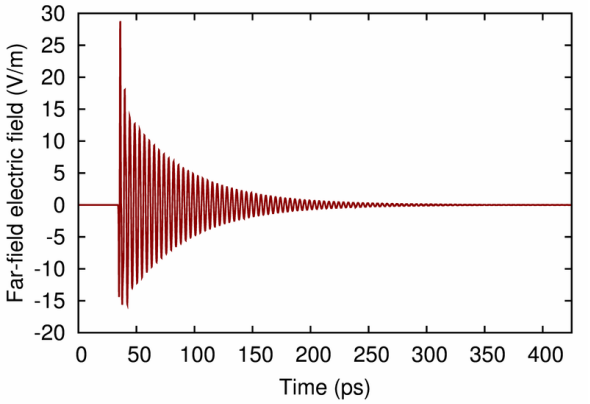

(c) $w = 0.750\lambda$.

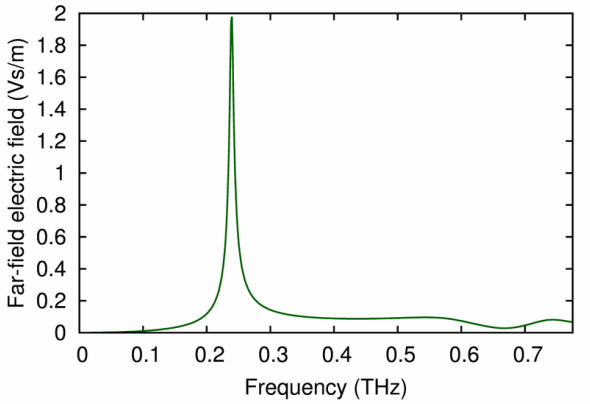

(d) $w = 0.750\lambda$.

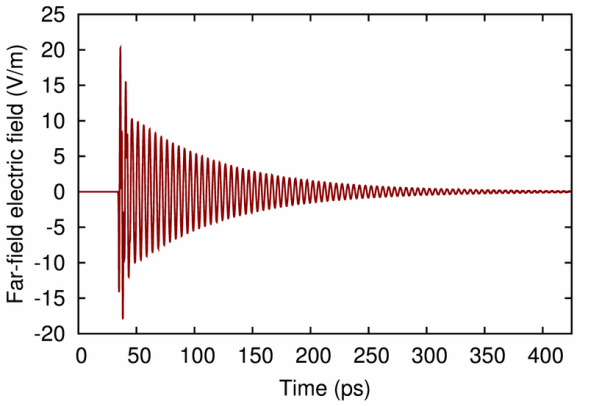

(e) $w = 1.000\lambda$.

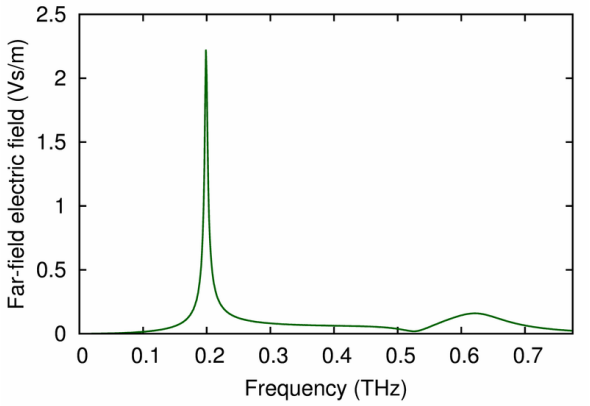

(f) $w = 1.000\lambda$.

Figure 3.6: Radiated far-field electric field pulse in the time and frequency domains for $w = 0.500\lambda, 0.750\lambda$ and $w = 1.000\lambda$.